On Building D-Stable Macromodels

Original
On Building D-Stable Macromodels / Bradde, T., Grivet-Talocia, S.. - ELETTRONICO. - (2026), pp. 1-4. (2026 IEEE 30th Workshop on Signal and Power Integrity (SPI) Turin (Ita) 14-17 June 2026) [10.1109/spi68887.2026.11594656].

Availability:
This version is available at: 11583/3013141 since: 2026-07-15T13:29:33Z

Publisher:
IEEE

Published
DOI:10.1109/spi68887.2026.11594656

(Article begins on next page)

On Building D-Stable Macromodels

Tommaso Bradde*, Stefano Grivet-Talocia*,
*Dept. Electronics and Telecommunications, Politecnico di Torino, Italy
tommaso.bradde@polito.it

***Abstract*—Vector Fitting (VF) is a widespread algorithm for building macromodels of complex linear time invariant electromagnetic components. One of the main reasons for its success is the possibility of easily enforcing model stability, a requirement that is essential for transient analysis. In this contribution, we generalize the standard VF stability enforcement through a novel rational fitting algorithm that enforces $\mathcal{D}$-stability, by placing the macromodel poles within arbitrary convex regions of the complex plane. The method is practically applied to improve the performance of VF in the presence of noisy data and to remove unwanted out-of-band poles.**

I. Introduction

Vector Fitting (VF) [1] is currently the main algorithm for the generation of accurate macromodels and equivalent circuits of complex electromagnetic structures described in terms of sampled Network Functions (NF). Virtually all commercial Computer Aided Design (CAD) tools focusing on signal and power integrity analyses provide users their own version of this algorithm due to its robustness, efficiency, and effectiveness for speeding up computationally demanding transient analyses.

One of the main reasons for the success of VF is the possibility of easily imposing the asymptotic stability of the resulting equivalent circuit, since this feature is essential for transient analysis [2]. Compared with other similar state-of-the-art techniques based e.g. on interpolation of the target NF [3], VF follows an iterative optimization process in which the poles of the underlying rational model representation are iteratively estimated by solving a small eigenvalue problem. Any unstable pole estimated in this way is simply mirrored to the left-half of the complex plane to guarantee the asymptotic stability of the resulting rational model.

Although effective for the enforcement of stability, the pole relocation step implemented in VF does not allow users to constrain the location of the macromodel poles to regions that differ from the left-half complex plane. However, the availability of a more precise pole placement algorithm would enable the construction of more robust and/or reliable macromodels. Two notable scenarios that are often advocated in applications involve preventing the occurrence of out-of-band poles [4] (which may lead to uncontrolled spurious dynamics as well as difficulties in passivity enforcement algorithms) or poles that are too close to the imaginary axis (often arising in presence of noise in the input data).

In this contribution, we introduce a modified VF scheme that constrains the poles of the resulting rational model within a general *Linear Matrix Inequality (LMI) region* of the complex plane, rather than restricting them solely to the left-half plane. This class of regions can approximate, with arbitrary precision, any convex set that is symmetric about the real axis [5]. Linear Time-Invariant (LTI) systems with poles confined to such regions are referred to as $\mathcal{D}$-stable [5]. Building upon recent developments in asymptotic stability within the interpolatory AAA framework [6], we enhance the VF optimization by incorporating explicit pole location constraints. Following the approach in [6], the resulting optimization problem is reformulated as a convex semidefinite program through a relaxation enabled by a weighted cost function, that is iteratively minimized during the fitting process.

We show experimentally how the proposed approach can be effectively applied to improve the performance of VF in presence of noisy samples and to avoid the presence of out-of-band poles in the macromodel.

II. Notation and Problem Statement

Most of the notation used in the paper is standard. We highlight that bold letters will be used for vectors and matrices, whose size will be always made explicit (e.g. $\mathbf{x} \in \mathbb{R}^n$ and $\mathbf{X} \in \mathbb{R}^{n\times n}$). The matrix $\mathbf{A}^T$ is the transpose of $\mathbf{A}$. The notation $\mathbf{A}\otimes\mathbf{B}$ denotes the Kronecker product of $\mathbf{A}$ and $\mathbf{B}$. The symbol $\mathbf{I}_n$ denotes the identity matrix of size n. Writing $\mathbf{J} \succ \mathbf{K}$ ($\mathbf{J} \succeq \mathbf{K}$) means that the matrix $\mathbf{J}-\mathbf{K}$ is positive (semi)definite. A collection of numbers indexed by subscript k, e.g. x_k with $1 \le k \le K$, will be shortly denoted as $\{x_k\}$.

We consider the following problem: given a collection of (possibly noisy) samples $\{\hat{\mathbf{H}}_k\}$ representing the NF of a P-port complex electromagnetic structure retrieved at a set of locations $\{s_k\}$ over the complex plane, our objective is to fit the available data to a rational function

$$\mathbf{H}(s) = \sum_{i=1}^{n} \frac{\mathbf{R}_i}{s-p_i} + \mathbf{R}_\infty, \tag{1}$$

such that:

C.1 the order n of the rational approximation is as small as possible

C.2 $\mathbf{H}(s) \approx \hat{\mathbf{H}}(s)\, \forall s \in \{s_k\}$

C.3 $\{p_i\} \subset \mathcal{D}$, where $\mathcal{D}$ is an arbitrary convex region of the complex plane that is symmetric with respect to the real axis.

A set with the properties of $\mathcal{D}$ is known as a Linear Matrix Inequality (LMI) region [5], [7] defined as

$$\mathcal{D} = \{s \in \mathbb{C} : \mathbf{L} + s\mathbf{M} + s^*\mathbf{M}^T \prec 0\}, \tag{2}$$

where $\mathbf{L} = \mathbf{L}^T$ and $\mathbf{M}$ are real matrices that uniquely determine the region. LMI regions of particular interest are, e.g., half planes, disks, cones, and strips.

III. Background: Vector Fitting

We review here the basic VF iteration, for an in-depth analysis of the algorithm see [1]. Given the model structure (1), the approximation condition **C.2** is enforced by optimizing the model unknowns $\{p_i\}, \{\mathbf{R}_i\}, \mathbf{R}_\infty$ to fit the available data samples in a least-squares sense. This is done by iteratively representing (1) in barycentric form as

$$\mathbf{H}^{(\mu)}(s) = \frac{\mathbf{N}^{(\mu)}(s)}{D^{(\mu)}(s)}, \quad \mathbf{N}^{(\mu)}(s) = \mathbf{\Gamma}_0^{(\mu)} + \sum_{i=1}^{n} \frac{\mathbf{\Gamma}_i^{(\mu)}}{s - q_i^{(\mu)}}, \quad (3)$$

and

$$D^{(\mu)}(s) = 1 + \sum_{i=1}^{n} \frac{\delta_i^{(\mu)}}{s - q_i^{(\mu)}} \quad (4)$$

where μ is the current iteration and $\mathbf{H}^{(\mu)}(s)$ is the corresponding representation of $\mathbf{H}(s)$, expressed in terms of the unknown coefficients $\mathbf{\Gamma}_0^{(\mu)}, \{\mathbf{\Gamma}_i^{(\mu)}\}, \{\delta_i^{(\mu)}\}$ and the instrumental (known) "basis" poles $\{q_i^{(\mu)}\}$. Each iteration performs the optimization of the current unknowns and an update of the poles $\{q_i^{(\mu)}\}$. Upon convergence of $\{q_i^{(\mu)}\}$, a linear least-squares estimation is performed to return $\mathbf{H}(s)$ in pole-residue form, as in (1).

Optimization. The optimization stage performs the enforcement of the requirement $\mathbf{H}^{(\mu)}(s) \approx \mathbf{H}(s) \forall s \in \{s_k\}$. To overcome the difficulties of solving the associated nonlinear least-squares problem, the condition is relaxed as

$$\mathbf{N}^{(\mu)}(s) \approx \hat{\mathbf{H}}(s) D^{(\mu)}(s) \quad \forall s \in \{s_k\}, \quad (5)$$

that is linear in the unknowns of the current iteration. The resulting least-squares problem is manipulated via the QR-based preprocessing introduced in [8], which eliminates the numerator unknowns $\mathbf{\Gamma}_0^{(\mu)}$ and $\{\mathbf{\Gamma}_i^{(\mu)}\}$ and produces an optimization problem in terms of the denominator coefficients $\{\delta_i^{(\mu)}\}$ only. These unknowns are found by solving a problem of the form

$$\min_{\tilde{\mathbf{C}}^{(\mu)}} \left\| \mathbf{G} \tilde{\mathbf{C}}^{(\mu)T} - \tilde{\mathbf{b}} \right\|_2^2, \quad (6)$$

where $\tilde{\mathbf{C}}^{(\mu)}$ collects the denominator variables as

$$\tilde{\mathbf{C}}^{(\mu)} = [\delta_1^{(\mu)}, \delta_2^{(\mu)}, \ldots, \delta_n^{(\mu)}] \in \mathbb{R}^{1 \times n} \quad (7)$$

while $\mathbf{G}$, $\tilde{\mathbf{b}}$ are a data matrix and a data vector. Notice that the number of unknowns of (6) does not depend on the number of electrical ports.

Pole Relocation. The objective of this step is to update the basis poles $\{q_i^{(\mu)}\}$ defining the model structure (3). The basis poles at iteration $\mu+1$ are chosen as the actual poles of $\hat{\mathbf{H}}^{(\mu)}(s)$. These poles can be computed once the optimal value of $\tilde{\mathbf{C}}^{(\mu)}$ is obtained by solving (6), since they coincide with the zeros of $D^{(\mu)}(s)$ in (4). From the numerical standpoint, they are found by solving a small eigenvalue problem that is formulated based on the state-space representation of the denominator

$$D^{(\mu)}(s) = \tilde{\mathbf{C}}^{(\mu)} (s\mathbf{I} - \tilde{\mathbf{A}}^{(\mu)})^{-1} \tilde{\mathbf{B}}^{(\mu)} + 1. \quad (8)$$

In the above, $\tilde{\mathbf{A}}^{(\mu)}$, $\tilde{\mathbf{B}}^{(\mu)}$, are known matrices while $\tilde{\mathbf{C}}^{(\mu)}$ is the solution of (6). By applying standard state-space inversion formulas, one checks that the zeros $D^{(\mu)}(s)$ are the eigenvalues of the matrix $\tilde{\mathbf{A}}^{(\mu)} - \tilde{\mathbf{B}}^{(\mu)} \tilde{\mathbf{C}}^{(\mu)}$. Hence the pole relocation step performs the assignment

$$\{q_i^{(\mu+1)}\} \equiv \text{eig}\{\tilde{\mathbf{A}}^{(\mu)} - \tilde{\mathbf{B}}^{(\mu)} \tilde{\mathbf{C}}^{(\mu)}\}. \quad (9)$$

To enforce the asymptotic stability of the model, the updated basis poles exhibiting a positive real part are simply flipped to the left-half complex plane. No further control is allowed on the poles location.

Residues Optimization. Ideally, the optimization and the relocation steps are repeated until VF converges to a fixed estimate of the model poles, that is when $\{q_i^{(\mu+1)}\} = \{q_i^{(\mu)}\}$, which is equivalent to $\tilde{\mathbf{C}}^{(\mu)} = \mathbf{0}$. Assuming this condition vierified at iteration $\bar{\mu}$, the algorithm performs the assignment

$$\{p_i\} \leftarrow \{q_i^{(\bar{\mu})}\} \quad (10)$$

in model structure (1). Once the poles of $\mathbf{H}(s)$ are fixed, the residues $\{\mathbf{R}_i\}$ and the direct coupling $\mathbf{R}_\infty$ are estimated by solving an additional least-squares problem. Different termination criteria can be applied in case convergence is not met, not discussed here. In the following we will denote the last VF iteration as $\bar{\mu}$.

IV. Enforcing $\mathcal{D}$-stability

Our main contribution is a strategy that constrains the pole relocation step (9) to place the updated basis poles over a prescribed $\mathcal{D}$ region of the complex plane. The starting point for our derivations is the following theorem, proved in [5]:

Theorem 1. *Given an LMI region*

$$\mathcal{D} = \{s \in \mathbb{C} : \boldsymbol{L} + s\boldsymbol{M} + s^* \boldsymbol{M}^T \prec 0\}$$

with $\boldsymbol{L} = \boldsymbol{L}^T$ and $\boldsymbol{M}$ real matrices and a matrix $\boldsymbol{X}$, it holds $\text{eig}\{\boldsymbol{X}\} \subset \mathcal{D}$ *if and only if there exists a symmetric matrix $\boldsymbol{Q} \succ 0$ such that*

$$\boldsymbol{L} \otimes \boldsymbol{Q} + \boldsymbol{M} \otimes (\boldsymbol{X}\boldsymbol{Q}) + \boldsymbol{M}^T \otimes (\boldsymbol{X}\boldsymbol{Q})^T \prec 0. \quad (11)$$

Theorem (1) provides the necessary and sufficient conditions for embedding the eigenvalue spectrum of a given matrix $\mathbf{X}$ in a prescribed LMI region $\mathcal{D}$. Hence, the problem of $\mathcal{D}$-stability enforcement can be solved by applying this theorem to the matrix involved in the pole relocation problem (9). We have the following as an immediate consequence

Proposition 1. *Let $\mathcal{D}$ be an LMI region defined as in Theorem 1, and let μ be an arbitrary VF iteration. Under the barycentric model representation* (3) *and the state-space realization* (8)*, it holds*

$$\{q_i^{(\mu+1)}\} \subset \mathcal{D} \quad (12)$$

if and only if there exists $\boldsymbol{Q} \succ 0$ such that

$$\begin{aligned} \boldsymbol{L} \otimes \boldsymbol{Q} &+ \boldsymbol{M} \otimes (\tilde{\boldsymbol{A}}^{(\mu)} \boldsymbol{Q} - \tilde{\boldsymbol{B}}^{(\mu)} \tilde{\boldsymbol{C}}^{(\mu)} \boldsymbol{Q}) \\ &+ \boldsymbol{M}^T \otimes (\tilde{\boldsymbol{A}}^{(\mu)} \boldsymbol{Q} - \tilde{\boldsymbol{B}}^{(\mu)} \tilde{\boldsymbol{C}}^{(\mu)} \boldsymbol{Q})^T \prec 0. \quad (13) \end{aligned}$$

The model $\boldsymbol{H}(s)$ is $\mathcal{D}$-stable if (13) *is verified at the last VF iteration $\mu = \bar{\mu}$.*

The above result shows that $\mathcal{D}$-stability enforcement boils down to the verification of the matrix inequality condition (13), expressed in terms of the denominator coefficients in vector $\tilde{\mathbf{C}}^{(\mu)}$. In standard VF, these coefficients are found in an unconstrained manner by solving (6). In order to enforce $\mathcal{D}$-stability, VF must be modified so that the optimal solution vector $\tilde{\mathbf{C}}^{(\mu)}$ verifies (13) by construction. This property can be enforced exactly by replacing problem (6) with the following constrained optimization problem (in which we drop the iteration index μ for readability)

$$\min_{\tilde{\mathbf{C}},\mathbf{Q}} \left\| \mathbf{G}\tilde{\mathbf{C}}^T - \tilde{\mathbf{b}} \right\|_2^2 \tag{14}$$

$$\text{subject to :}$$

$$\mathbf{Q} = \mathbf{Q}^T \succ 0$$

$$\mathbf{L} \otimes \mathbf{Q} + \mathbf{M} \otimes (\tilde{\mathbf{A}}\mathbf{Q} - \tilde{\mathbf{B}}\tilde{\mathbf{C}}\mathbf{Q}) + \mathbf{M}^T \otimes (\tilde{\mathbf{A}}\mathbf{Q} - \tilde{\mathbf{B}}\tilde{\mathbf{C}}\mathbf{Q})^T \prec 0.$$

Unfortunately, the above problem involves a matrix inequality that is bilinear in the variables $\tilde{\mathbf{C}}$ and $\mathbf{Q}$. The techniques that are available to tackle this kind of problems either do not guarantee global optimality or can be practically applied only in case of very few variables. Hence, we propose to apply a convex relaxation of (14) in order to make the resulting fitting scheme robust and efficient.

The strategy that we pursue is inspired by the one introduced in [6, Sec. 4.3] to enforce asymptotic stability in the well-known Adaptive-Antoulas-Anderson (AAA) algorithm. We omit the details of the derivation and we present the final result, which is cast as the following constrained optimization problem in epigraph form

$$\min_{t,\mathbf{Q},\boldsymbol{\delta}} t \tag{15a}$$

$$\text{subject to :} \tag{15b}$$

$$\mathbf{Q} = \mathbf{Q}^T \succ 0 \tag{15c}$$

$$\mathbf{L} \otimes \mathbf{Q} + \mathbf{M} \otimes (\mathbf{A}\mathbf{Q} - \mathbf{B}\boldsymbol{\delta}) + \mathbf{M}^T \otimes (\mathbf{A}\mathbf{Q} - \mathbf{B}\boldsymbol{\delta})^T \prec 0, \tag{15d}$$

$$\begin{bmatrix} t & (\boldsymbol{\delta}^T - \mathbf{Q}\mathbf{b})^T \\ (\boldsymbol{\delta}^T - \mathbf{Q}\mathbf{b}) & \mathbf{Q} \end{bmatrix} \succeq 0. \tag{15e}$$

The various matrices in (15) are derived from (14) by computing the "thin" SVD of $\mathbf{G} = \mathbf{U}\boldsymbol{\Sigma}\mathbf{V}^T$ and performing a change of variable through a similarity transformation

$$\mathbf{A} = \mathbf{T}^{-1}\tilde{\mathbf{A}}\mathbf{T},\ \mathbf{B} = \mathbf{T}^{-1}\tilde{\mathbf{B}},\ \mathbf{C} = \tilde{\mathbf{C}}\mathbf{T},\ \mathbf{b} = \mathbf{U}^T\tilde{\mathbf{b}},\ \mathbf{C}\mathbf{Q} = \boldsymbol{\delta} \tag{16}$$

with $\mathbf{T} = \mathbf{V}\boldsymbol{\Sigma}$.

It can be shown that (15) is equivalent to (14) up to a weighting of the involved least-squares residues via the matrix $\mathbf{Q}$. Experimental evidence shows that such weighting does not impair the accuracy of the fitting, see Sec. V. Contrarily to (14), problem (15) is convex and can be solved efficiently by means of off-the-shelf semidefinite programming solvers.

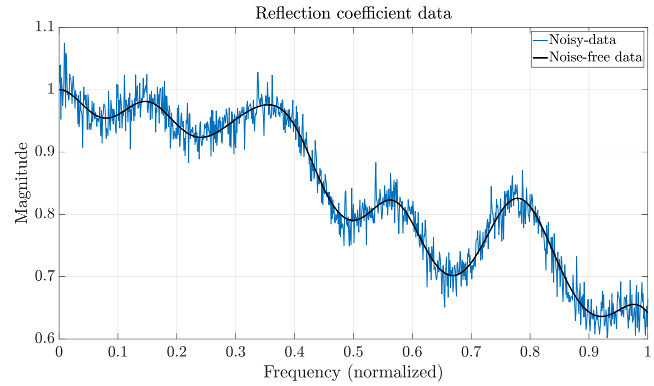

Fig. 1. The magnitude of the reflection coefficient of a transmission line network. Black line: reference data obtained via virtual measurements. Blue line: the same data corrupted by synthetic Gaussian noise.

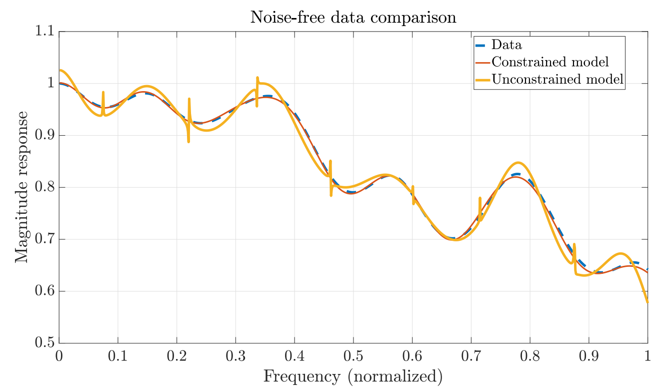

Fig. 2. Comparison between the noise-free data (blue line) of the reflection coefficient and two models built using the noise-corrupted data. Yellow line: the model obtained by applying unconstrained VF. Spurious resonances appear due to the presence of noise (not shown here). Red line: the model obtained by applying the proposed constrained VF iteration.

V. Numerical Results

We first apply the proposed methodology to approximate the reflection coefficient of a transmission line network originally introduced in [9], considering the presence of noise in the available data. A set of reference virtual measurements of the reflection coefficient is generated using an in-house Matlab code that integrates a quasi-static 2D field solver for the extraction of transmission line parameters and a frequency-domain solution of the distributed network over the bandwidth $[50, 1000]$ MHz. Within this frequency range, a total of $K = 1000$ samples $\hat{\mathbf{H}}_k$ are collected. These noiseless data are depicted in black in Fig. 1.

Additive noise $\nu_k = \nu_{\text{Re},k} + j\nu_{\text{Im},k}$ is then introduced into each transfer function sample $\hat{\mathbf{H}}_k$, where both $\nu_{\text{Re},k}$ and $\nu_{\text{Im},k}$ are random variables drawn from zero-mean Gaussian distributions. The variance of these random variables is normalized such that the RMS value of the noise vector $\boldsymbol{\nu} = [\nu_1, \nu_2, \ldots \nu_{1000}]$ is $\boldsymbol{\nu}_{\text{RMS}} = 0.03$, corresponding to 3.5% of the RMS value of the reference data. The resulting noise-contaminated magnitude of the reflection coefficient is illustrated in Fig. 1 (blue line). Applying the standard VF

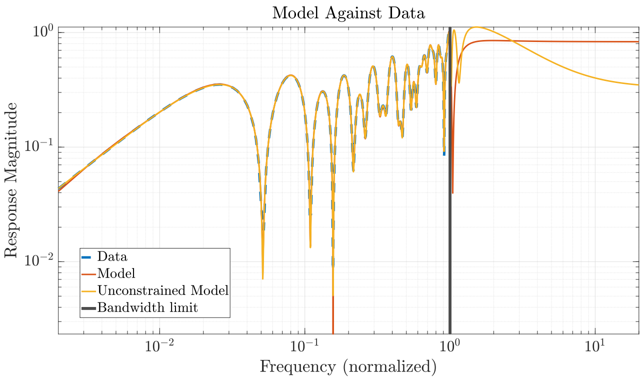

Fig. 3. Fitting of a PCB transmission coefficient. Yellow line: unconstrained fitting. Red line: enforcing only in-band poles (data are available up to 1 in the normalized frequency scale).

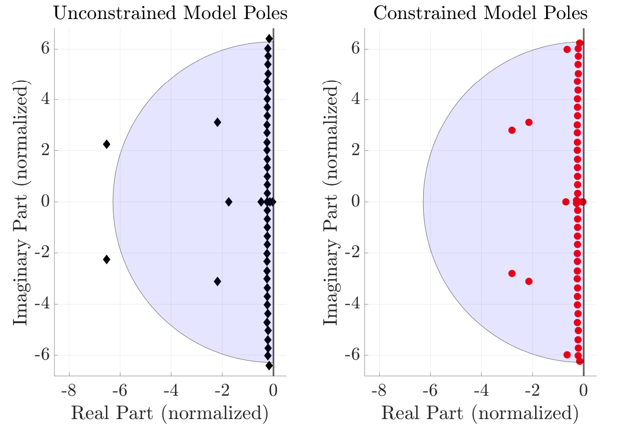

Fig. 4. Left: the poles of a macromodel that exhibits out-of-band poles. Right: the poles are relocated within the bandwidth applying the proposed approach.

algorithm to the noisy dataset with a model order set to $n = 25$ yields the approximation shown in Fig. 2 (yellow line) after 20 iterations. The approximation quality is substantially degraded by the presence of noise, which results in the identification of spurious undamped poles. The proposed approach is therefore applied to force the model poles to lie within the left-half complex plane defined by $\mathfrak{Re}\{s\} < -\alpha < 0$, with the objective of eliminating these artificial resonances. This constraint is imposed by selecting $\mathbf{L} = 2\alpha$ and $\mathbf{M} = 1$ in the constraints of problem (15), which specifies the $\mathcal{D}$-region as

$$\mathcal{D} = \{s \in \mathbb{C} : 2\alpha + s + s^* = 2\sigma + 2\alpha < 0\}. \qquad (17)$$

We set $\alpha = 0.8$ based on grid-search and we applied the proposed approach by constraining 20 VF iterations. The magnitude response of the constrained model obtained is displayed in Fig. 2 (dashed-blue line). The proposed constrained fitting strategy significantly outperforms the unconstrained approach and effectively suppresses the nonphysical resonances of the reduced-order model. The constrained model is built in approximately 20 s on a workstation equipped with 32 GB RAM and a 3.3 GHz Intel i9-X7900 CPU.

A second experiment shows how the proposed approach can be used to avoid out-of-band poles in the macromodel. We model the reflection coefficient of the high-speed Printed Circuit Board (PCB) interconnect introduced in [10], across the the bandwidth $[0.01, 10]$ GHz. A model of order $n = 51$ was built using standard VF, terminated after 20 iterations. The yellow line of Fig. 3 shows that the resulting model exhibits out-of-band poles. Such poles are removed by performing an additional constrained iteration, using the proposed approach. To this aim, we require the poles to fall into the left-half disk centered at the origin and having radius equal to the prescribed bandwidth limit, as in Fig. 4. This strategy effectively removes the unwanted poles and the out-of-band passivity violations, without impairing the accuracy of the model as shown by the red line of Fig. 3. The model was generated in ≈ 6.5 s.

VI. Conclusions

We presented a novel approach to constrain the location of the poles of macromodels obtained via the VF algorithm. Applying the proposed method, the poles can be placed over arbitrary convex regions of the complex plane that are symmetric with respect to the real axis. The main technical enabling factor is the solution of a relaxed semidefinite program derived from the exact non-convex conditions required by the theory of $\mathcal{D}$-stability. We shown how the approach can be applied to improve the performance of VF in presence of noisy data and to remove poles falling beyond the modeling bandwidth limit.

References

[1] B. Gustavsen and A. Semlyen, "Rational approximation of frequency domain responses by vector fitting," *IEEE Transactions on Power Delivery*, vol. 14, no. 3, pp. 1052–1061, 1999.

[2] T. Bradde, S. Grivet-Talocia, A. Zanco, and G. C. Calafiore, "Data-driven extraction of uniformly stable and passive parameterized macromodels," *IEEE Access*, vol. 10, pp. 15 786–15 804, 2022.

[3] Y. Nakatsukasa, O. Sete, and L. N. Trefethen, "The AAA algorithm for rational approximation," *SIAM J. Sci. Comput.*, vol. 40, no. 3, pp. A1494–A1522, 2018.

[4] S. Grivet-Talocia and A. Ubolli, "On the generation of large passive macromodels for complex interconnect structures," *IEEE Transactions on Advanced Packaging*, vol. 29, no. 1, pp. 39–54, 2006.

[5] M. Chilali and P. Gahinet, "$\mathcal{H}_\infty$ design with pole placement constraints: an LMI approach," *IEEE Transactions on Automatic Control*, vol. 41, no. 3, pp. 358–367, 1996.

[6] T. Bradde, S. Grivet-Talocia, Q. Aumann, and I. V. Gosea, "A modified aaa algorithm for learning stable reduced-order models from data," *Journal of Scientific Computing*, vol. 103, no. 1, p. 14, 2025.

[7] M. Chilali, P. Gahinet, and P. Apkarian, "Robust pole placement in LMI regions," *IEEE Transactions on Automatic Control*, vol. 44, no. 12, pp. 2257–2270, 1999.

[8] D. Deschrijver, M. Mrozowski, T. Dhaene, and D. De Zutter, "Macromodeling of multiport systems using a fast implementation of the vector fitting method," *Microwave and Wireless Components Letters, IEEE*, vol. 18, no. 6, pp. 383–385, june 2008.

[9] E. Fevola, A. Zanco, S. Grivet-Talocia, T. Bradde, and M. De Stefano, "An adaptive sampling process for automated multivariate macromodeling based on hamiltonian-based passivity metrics," *IEEE Transactions on Components, Packaging and Manufacturing Technology*, vol. 9, no. 9, pp. 1698–1711, 2019.

[10] J. B. Preibisch, B. Jayaprakash, T. Reuschel, K. Scharff, B. Sen, and C. Schuster, "Exploring efficient variability-aware analysis method for high-speed digital link design using pce," in *Proc. UBM DesignCon*, Santa Clara, CA, USA, 2017. [Online]. Available: https://www.signalintegrityjournal.com/articles/699-designcon-personal-reflections-on-the-past-twenty-years